SOME ASPECTS OF MOVING-BASE SIMULATION OF UPSET RECOVERING MANEUVER

L.E.Zaichik, Y.P.Yashin, P.A.Desyatnik*
***The Central Aerohydrodynamic Institute (TsAGI), Zhukovsky, Russia**
zaichik@tsagi.ru

Keywords: *upset recovery, simulation, drive algorithms, motion perception*

Abstract

Considered are some aspects of motion cueing on hexapods in simulation of upset/stall recovering maneuver, as a result of project SUPRA of the 7th European Framework Program.

Inadequate motion cueing or large motion cues distortions can distort pilot's opinion about the maneuver and affect training results. In the paper, the main attention is paid to motion fidelity aspects, which are determined, on the one hand, by the accuracy of the "useful" motion cues reproduction and, on the other hand, by inevitable false cues. On the basis of the experimental data on the effect of large G-loads on pilot's perception of angular and linear motion and the data available on the motion fidelity criteria [1,2,3], the methods are discussed to optimize (adapt) the "classical" filters for the upset recovery simulation.

The results of the optimizations are tested in experiments with test pilots. The objective and subjective measurements received in the experiments demonstrate both the effectiveness of the proposed optimization and the need to conduct pilot training on moving-base hexapod-type simulators.

1 Introduction

Recent years, the loss of control became the reason for the most of flight accidents. A more recent safety review [4] listed loss-of-control as the most common category of fatal accidents in the period 1997-2006, accounting for 2573 fatalities world-wide. It can be fully attributed to a lack of pilots' training of adequate control actions to recover from the upsets and stalls. Thus, the development of methods and tools of pilots' upset recovery training is the task of supreme importance. The task was the goal of project "SUPRA" of the 7th European Framework Program. Some of the results received within the project are shown in the presented paper.

On-ground simulation of critical flight modes is a challenging problem, which requires a number of non-trivial tasks to be solved. One of them is reproduction of motion cues arising in upsetting and upset recovering. At present, the most of aviation training centers are equipped with simulators of hexapod-type. On such simulators, the simulation of the critical flight modes is limited by the fact the motion cues the pilot perceives during stalling, spinning and upset recovering can not be adequately reproduced.

Development and optimization of any motion drive algorithms are usually based the regularities of acceleration perception and the role of motion cues in piloting. It is known that G-loads up to 2.0-2.5 g arise during the upset recovery maneuver. One of the most significant deficiencies of hexapod-type simulators, in terms of upset recovering simulation, is impossibility to reproduce considerable low-frequency G-loads. On the other hand, as earlier publications show [5,6], normal G-load can affect the motion perception along other degrees of freedom (DoF). Therefore, the questions arise: how strong is G-load effect and how to take it into account? The lack of sufficient data on this question was, seemingly, the reason for the available guidance to train flight crews [7] does not give any requirements for motion cueing. As a result, the crews are often trained on fixed-based simulators, though the lack of accelerations or their inadequate reproduction may be one of the main sources of training errors.

2 Peculiarities of Motion Cueing in Upset Recovery Simulation

The aircraft upset/stall is a rare, but very dangerous event. The majority of the pilots have never experienced such an event and have no idea about the nature of the motion cues arising in upset and upset recovering. Inadequate motion cueing or motion distortions introduced by drive algorithms can distort pilot's opinion and affect pilot training. That is why the motion fidelity in simulation of upset recovery maneuver is of great importance.

At present, most of hexapod-type simulators use so-called "classical" drive algorithms based on washout filters. The algorithms allow adequate reproduction of motion cues arising during standard flight modes of transport aircraft. Their many-years using has contributed to algorithms improvement and to development of multiple motion fidelity criteria [1-3]. Thus is would be worthwhile to apply, first of all, the collected knowledge about "classical" algorithms for their adaptation to upset recovering simulation.

Table 1

Degree of freedom	**max value**	**min freq (*rad/s*)**
Vertical	2.5 *g*	<0.2
Longitudinal	0.15 *g*	<0.2
Lateral	0.2 *g*	1.0-2.0
Roll	40 *deg/s*	1.0-2.0
Pitch	15 *deg/s*	1.0-2.0
Yaw	10 *deg/s*	1.0

Table 1 presents the maximum values and minimum frequencies of the flight parameters, which are, in the same time, the main sources of motion information for the pilot. The data were received while simulating (with SUPRA aircraft model) of various upset scenarios. The presented data are in accordance with the other data received in flight and taken from publications [8].

It is seen that all flight parameters are of very low frequencies. It is known that reproduction of the low-frequency motion cues on hexapod simujlators is either accompanied by distortions or impossible due to simulator technical limitations. Figure 1 presents technical limitations of benchmark hexapod simulator as a function of the motion cues frequency, as well as the boundaries of the false cues (for angular DoF). It is seen that the most "problematic" DoF in terms of upset recovery simulation are heave and roll. In addition to that shown in Figure 1, there are also limitations due to the cues of opposite sign [2]. Thus, a question arises: Is it possible to provide motion fidelity sufficient to simulate upset recovery maneuver?

The answer on the question is determined by the following factors: (1) accurate reproduction of the "useful" motion cues, and (2) minimizing of the false cues due to motion system drive algorithms.

3 Reproduction of the "Useful" Motion Cues

Any motion drive algorithms are based on the regularities of acceleration perception. It is known that upset recovery maneuver is characterized by low-frequency normal G-load of 2.0-2.5 g. The hexapod-type simulators have little capabilities to reproduce such G-loads. Nevertheless, the G-loads determine the reproduction of motion cues along other degrees of freedom.

3.1 Reproduction of Angular Motion

The data presented in [5,6] show that normal G-loads can affect the motion perception considerably. On hexapods, the effect of G-load can be studied only for small and high-frequency accelerations (with frequencies higher 1 rad/s). Thus, to analyze the effect of low-frequency normal accelerations we use in-flight data received in the course of SUPRA project and the data received earlier and described in [6].

The data are presented in Figure 2 for roll axis; the similar functions are available for pitch and yaw axis. It is seen that the normal G-loads noticeably affect angular motion perception. The function can be approximated by the following expression (for the roll):

$$p / p_0 = 1 + k \cdot \Delta n_z \,, \qquad (1)$$

where p_0 is the absolute threshold value at the particular frequency, Δn_z is normal acceleration increment.

Experiments were conducted for different frequencies of angular and linear motion: ω_{nz} = 0.5 rad/s, $\omega_{p,q}$ = 2 rad/s; ω_{nz} = 0.2 rad/s, $\omega_{p,q}$ = 0.5 rad/s. Nevertheless, the functions received appeared to be similar to each other regardless of the motion frequency. It means that coefficient k can be assumed independent of motion frequency and equal k=1.5.

According to (1), as normal G-load increases from 1 to 2.0-2.5 g, the angular motion thresholds increase by factor 2.

The data available in [5] allow approximation of function (1) for the perception of over-threshold angular rate perception.

These and other data formulate the basis for the algorithms adaptation. To reproduce the perception of angular motion affected by simultaneous vertical accelerations, an adaptive coefficient is implemented into angular motion cueing algorithm (high-pass filters paths), which reduces reproduced angular rates in accordance with the following expression:

$$k = \frac{1}{1 + 1.5\left|\Delta n_z\right|} \,.$$

3.2 Reproduction of Longitudinal and Lateral Accelerations

At present, there are no sufficient data on the effect of low-frequency normal G-load (typical of upset recovering) on the perception of linear accelerations in horizontal plane. Such data can be received on special simulators only. Thus, we need to make some hypothesis and assumptions. It was shown earlier [5], that linear accelerations are perceived by different sensory systems depending on acceleration frequencies. The low-frequency accelerations (about 0.2-2.0 rad/s) are perceived by vestibular system; as frequency increases over 2-4 rad/s, the absolute thresholds decrease (sensitivity increases), and the accelerations are perceived by kinesthetic and tactile sensors.

Thus, it is natural to assume that the effect of low-frequency normal G-load on the perception of linear longitudinal and lateral ("horizontal") accelerations depends on the frequency of the latter. If the frequencies of the horizontal accelerations are rather low and within the G-load frequency range (0.2-1.0 rad/s), their perception may be affected by large G-loads, since both of them are perceived by one and the same sensory system. If the frequencies of the horizontal accelerations are much higher than the G-load frequencies (>3 rad/s), the normal G-load should not noticeably affect the perception of the horizontal accelerations, since they are perceived by different sensory systems, and the sensitivity to high-frequency accelerations is higher.

Table 1 shows that the frequencies of the longitudinal accelerations practically coincide with frequencies of the normal G-loads, and frequencies of the lateral accelerations are much higher. Thus, the assumptions stated can be applied for the longitudinal accelerations, in the first place.

The peculiarities of the effect of G-load on longitudinal acceleration perception are easy to be taken into account by the classical washout filters: low-pass and high-pass filters provide dividing longitudinal accelerations according to their frequencies. The reduced sensitivity to longitudinal accelerations can be simulated in the low-pass filters by implementing weight coefficients $k=n_x/n_z$. The high-pass filters remain unchanged.

3.3 Reproduction of Normal Accelerations

In classical algorithms normal specific forces are reproduced by using high-pass filters only, and, as it was mentioned above, hexapod-type simulators have little capabilities to reproduce low-frequency G-loads. Nevertheless, it is possible to improve the reproduction of G-load gradient and to enhance the sensation of G-break.

To do this, a nonlinear coefficient can be introduced into the normal acceleration path with function shown in Figure 3. The nonlinear element amplifies the normal acceleration on the initial stage and limits its maximum. Figure 4 shows spectral density of the reproduced normal acceleration. It is seen that the nonlinear coefficient increases the high-frequency component of the G-load, which, according to pilots, leads to better sensation of G-break: (Pilot: "Sometimes I feel it").

4 Minimization of False Cues

The motion fidelity is sufficient if the false cues are eliminated or, at least, reduced to minimum. The minimization of false sensation is especially important in case of simulation of rare phenomenon for pilot training.

The plots in Figure 5 show how the simulator motion of the TsAGI PSPK-102 conventional hexapod simulator (output) corresponds to the actual aircraft motion (input) during a specific upset scenario ("a symmetric stall"). The aircraft data originates from the SUPRA aerodynamic model that was developed within SUPRA project with the manoeuvre flown by a test pilot in a fixed-base simulator. The simulator data was obtained using the conventional motion filter settings (optimized for the normal flight envelope) and the aircraft data as input. Please note that in the plots the conventional outputs are shown with gains set equal to 1 in order to make phase distortions and false cues more clear (usually, gains of classical washout filters are smaller than 1).

The comparison shows the following main distortions (the encircled numbers in figures correspond to the distortions):

1. There are phase distortions (e.g. time delays) in reproducing longitudinal (Nx) and lateral (Ny) accelerations; the lateral accelerations (Ny) is more problematic.
2. Angular motion is accompanied by large false cues due to high-pass filters, which is perceived as motion in opposite direction, in some cases exceeding the onset cues. The most problematic is the roll axis due to large angular rates and, as a consequence, large false cues. In addition to this type of false cues, there are also false specific forces due to cockpit tilting while reproducing angular motion (is not shown).

To avoid/minimize the listed distortions and false cues we need to properly select filter parameters, which can be done with the help of motion fidelity criteria developed in [1-3].

4.1 Selection of Filter Settings for Angular Motion

To proper select filter settings for angular motion a certain compromise should be found: on the one hand, we select filter frequency to better reproduce the "useful" cues and to stay within cockpit travel limitations; on the other hand, we have to minimize the arising false cues.

The selection of filter frequencies and gains can be done in accordance with the fidelity criteria [1-3], which reliability has been proved by their many-years using in various handling qualities and simulation studies. To better reproduce angular motion and to stay within the simulator travel limitations, we can use the curves shown in Figures 6 and 7.

Figure 6 shows the motion fidelity ratings (in percentage) as a function of high-pass filter frequencies (both for angular and linear motion): motion fidelity is 100% if ω_{hp}=0, corresponded to real flight conditions; motion fidelity is 0% if $\omega_{hp} \to \infty$, corresponded to fixed-base conditions. The Figure allows selection of high-pass filter frequencies in the better way.

Figure 7 allows selection of angular motion gain in order to stay within the cockpit travel limitations. The Figure shows motion fidelity ratings (in percentage) as a function of the root-mean-square of simulator angular rate. It is seen, in particular, that the good motion fidelity (>80%) can be achieved if the value of $\sigma_{p\ sim}$ is just three times greater than the angular rate threshold value (roll rate threshold value is 0.3 deg/s at frequencies 1-2 rad/s).

Unfortunately, false cues arising due to high-pass filters are inevitable. While modeling large-amplitude angular motion two types of false cues arise: the false specific forces due to cockpit tilting, and false cues of opposite sign. The two types of the false cues can arise independently or simultaneously depending on simulator travel capabilities. Their integrated effects on motion fidelity are shown in Figure 8. The data are functions of simulation fidelity ratings (MR – Motion Roughness, [2]) versus high-pass filter frequencies for various bank angles capture tasks without scaling. At low frequencies the simulation fidelity worsening is mainly due to false specific forces. Here, the cockpit tilt angles are almost equal to aircraft bank angles, while at the same time false opposite roll rates are insignificant. As the filter frequencies increase, the tilt angles and, consequently, the false lateral accelerations decrease, but the false roll rates opposite in sign increase; thus, as filter frequencies increase simulation fidelity is increasingly determined by false roll rates opposite in sign.

In accordance with the curves in Figure 8, the minimization of false cues effect can be done by adjusting the high-pass filter frequency or by downscaling the filter gain.

4.2 Selection of Filter Settings for Lateral Accelerations

The proper selection of filter settings for linear motion is a sort of compromise as well. The first selection is performed from point of view of better simulation of the useful cues (see Figures 6 and 7). The further adjusting is performed to minimize the inevitable false cues.

As it was said above, there are phase distortions in the reproduction of the horizontal accelerations. The effect of the distortions on motion fidelity depends on the motion cues frequency: the closer the motion cues frequency to the filter cutoff frequency, the stronger the distortion effect.

As it is seen from the Table 1, the longitudinal accelerations are mainly of very low frequencies about 0.2 rad/sec; the lateral accelerations are of higher frequency, about 1-2 rad/sec. Thus, selection of filter frequency equal 1.4 rad/sec can worsen the lateral acceleration reproduction. It is also confirmed by the plots in Figure 5: the distortions of Ny is more evident.

Figure 9 presents frequency responses as a sum of the low- and high-pass filters. It is seen that in the vicinity of the filter cutoff frequency (1.4 rad/sec) the accelerations are completely washed out. In other words, we do not reproduce the lateral accelerations at the substantial frequencies.

To improve the situation we propose to replace “classical” low-pass filter with a filter, which contains middle frequencies:

$$Y_{lp} = \frac{2\varsigma T \cdot K \cdot s + 1}{T^2 s^2 + 2\varsigma T s + 1}$$

It is seen from Figure 9 that the introduction of the complementary filter leads to noticeably decreasing of the “drop” in the lateral acceleration frequency response and, thus, decreasing of the phase distortions.

The gain K in the filter is selected with pilots to avoid jerky accelerations due to rapid cockpit rotation.

Thus, the optimization of drive algorithms allowed following improvements compared to the “classical” algorithms:

- The effect of G-loads is taken into account by introduction of adaptive coefficients into angular and linear motion reproduction paths;
- Nonlinear coefficient is implemented into high-frequency normal acceleration path in order to enhance the sensation of G-break;
- Complementary filter is introduced into low-frequency path of lateral accelerations in order to reduce the phase distortions;
- Filter settings are selected in accordance with the motion fidelity criteria to improve reproduction of “useful” cues and to minimize the false cues.

5 Simulation Results and Discussion

The optimized drive algorithms were tested in simulator experiments. Four test pilots participated in the experiments. Various upset/stall scenarios were considered. Two motion configurations were considered: “classical” algorithms and “optimized” algorithms.

The main goal of the experiments was to demonstrate the effectiveness of motion cueing on hexapod-type simulators.

First of all, it should be mentioned that all of the pilots appreciated the optimized algorithms: “The motion cues became more clear", "The motion helps, makes flying more vivid, forms a more complete image of flight".

The positive effect of cockpit motion is confirmed by objective measurements as well. Figures 10 and 11 show data received in fixed-base simulations and moving-base simulations with the optimized algorithms.

Data in Figure 10 are spectrum powers of the wheel displacements (in roll and pitch), and roll and pitch rates. It is the data for one pilot, averaged for 10 motion-off and 10 motion-on flights. Data in Figure 11 are standard deviations of wheel displacements and flight parameters for motion-on and motion-off cases. The similar data were received for all test pilots and for different upset/stall scenarios. Thus we can speak about the common regularities.

Figure 10 and 11 show that, despite of the lack of large normal G-loads on hexapods, the cockpit motion affects pilot's control activities and flight controlled parameters: the high-frequency components in the spectra decrease, standard deviations decrease. The effect is more evident in roll axis, which is in agreement with the data available on the effect of motion cues in piloting.

In accordance with the knowledge on the acceleration role in piloting [9], motion cues role is beneficial when they are the second derivative of the visually controlled parameter and their values are above the threshold value. In this case the motion cues help the pilot to control an aircraft, to more accurate shape the control inputs and, thus, positively assessed by pilots.

For the roll control the conditions for beneficial role of motion cues are met almost in all cases. Thus, the motion cues effect in roll control is more evident (see figure 10).

Analysis of the flight velocities in upset/stall recovering (Figure 12) shows that it is, mainly, pitch control which determines pilot activity in upset/stall recovering. But, as it is seen from Table 1, the pitch rates are not large and, moreover, their perception is suppressed by simultaneous G-loads. Thus, motion cueing in pitch and heave does not noticeably affect pilot's activities (see fig.10). The motion cues can cause just a certain "disciplinary" effect on pilot activity.

6 Conclusions

The paper presents some methods to optimize "classical" drive algorithms to adapt them to upset/stall recovery simulation. The main attention is paid to the effect of G-load on the perception of motion cues along other degrees of freedom, as well as to other aspects determining simulation fidelity.

The effectiveness of the developed optimization is demonstrated by both the objective measurements (frequency spectra, standard deviations) and pilot's subjective assessments.

The pilot training for upset recovery maneuver should be conducted on moving-base simulators.

References

[1] V.V.Rodchenko, A.D.White, "Motion Fidelity Criteria Based on Human Perception and Performance," *AIAA-99-4330*, Portland OR, 1999.

[2] L.E.Zaichik, Y.P.Yashin, P.A.Desyatnik, "Motion Fidelity Criteria for Large-Amplitude Tasks", *AIAA-2009-5916*, Chicago Il, 2009.

[3] L.E.Zaichik, Y.P.Yashin, P.A.Desyatnik, "Peculiarities of Motion Cueing for Precision Control Tasks and Maneuvers," *ICAS Paper 602*, Nice, France, 2010.

[4] EASA Safety Review 2006

[5] L.E.Zaichik, V.V.Rodchenko, Y.P.Yashin, I.V.Rufov, A.D.White. "Acceleration perception", *AIAA-99-4334*, Portland OR, 1999.

[6] A.D.White, V.V.Rodchenko, S.Yu.Boris, "In-Flight Estimation of Pilot's Acceleration Sensitivity Thresholds," *AIAA-2000-4292*, Denver CO, 2000.

[7] *Airplane Upset Recovery Training Aid. Industry Solutions for Large Swept-Wing Turbofan Airplanes Typically Seating More Than 100 Passengers*. Revision 2, November 2008.

[8] G.S.Kalachev. *Airplane, Pilot and Flight Safety*, M: Mashinostroyenie, 1979 (in Russian).

[9] B.P.Lee, V.V.Rodchenko, L.E.Zaichik, Y.P.Yashin, "Simulation-To-Flight Correlation", *AIAA-2003-5823*, Austin TX, 2003.

Copyright Statement

give permission, or have obtained permission from the copyright holder of this paper, for the publication and distribution of this paper as part of the ICAS2012 proceedings or as individual off-prints from the proceedings.

7 Figures

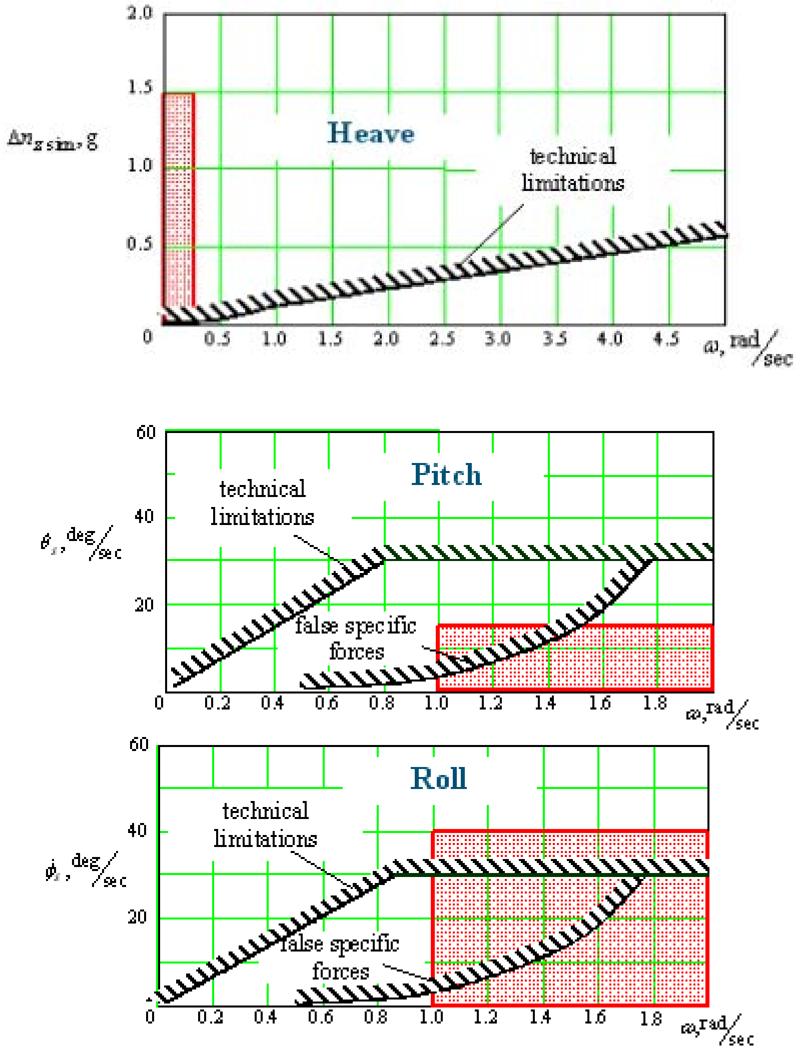

Fig. 1. Limitations for hexapod-type simulators to reproduce motion cues typical of upset recovering maneuver.

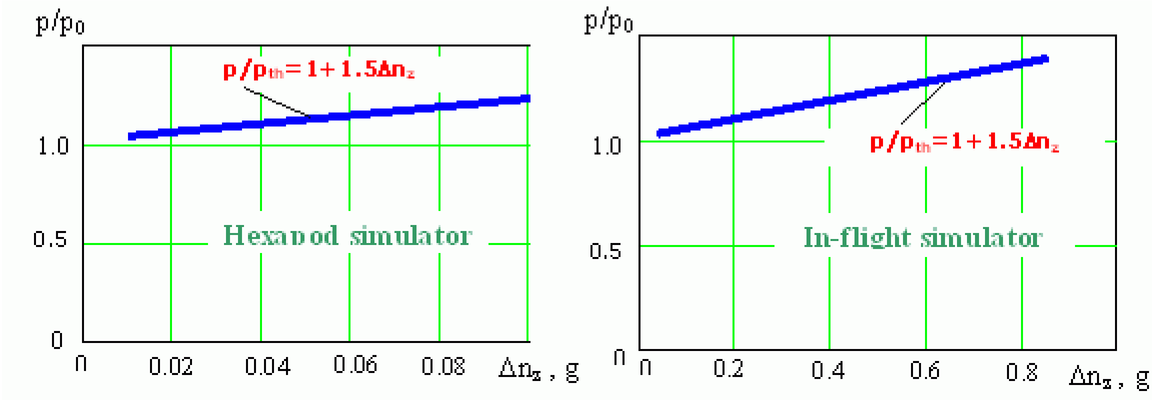

Fig. 2. Effect of normal G-load on the perception of angular motion.

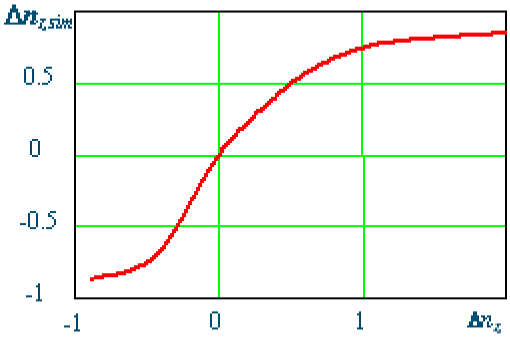

Fig. 3. The nonlinear gain in high-frequency path of normal acceleration.

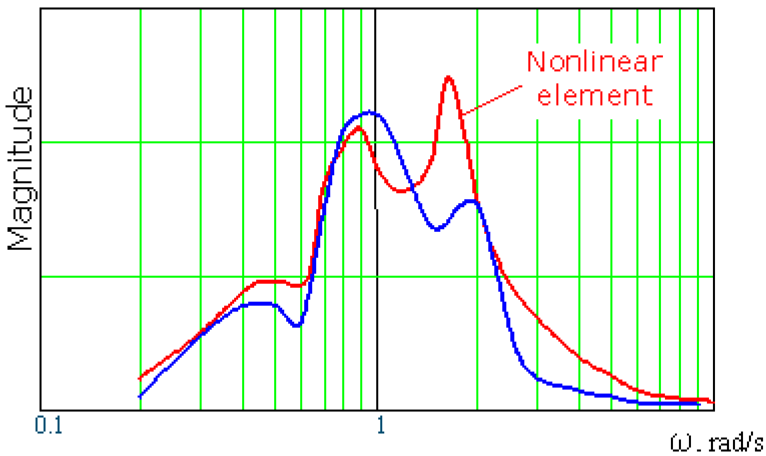

Fig. 4. Spectrum density of the reproduced normal accelerations.

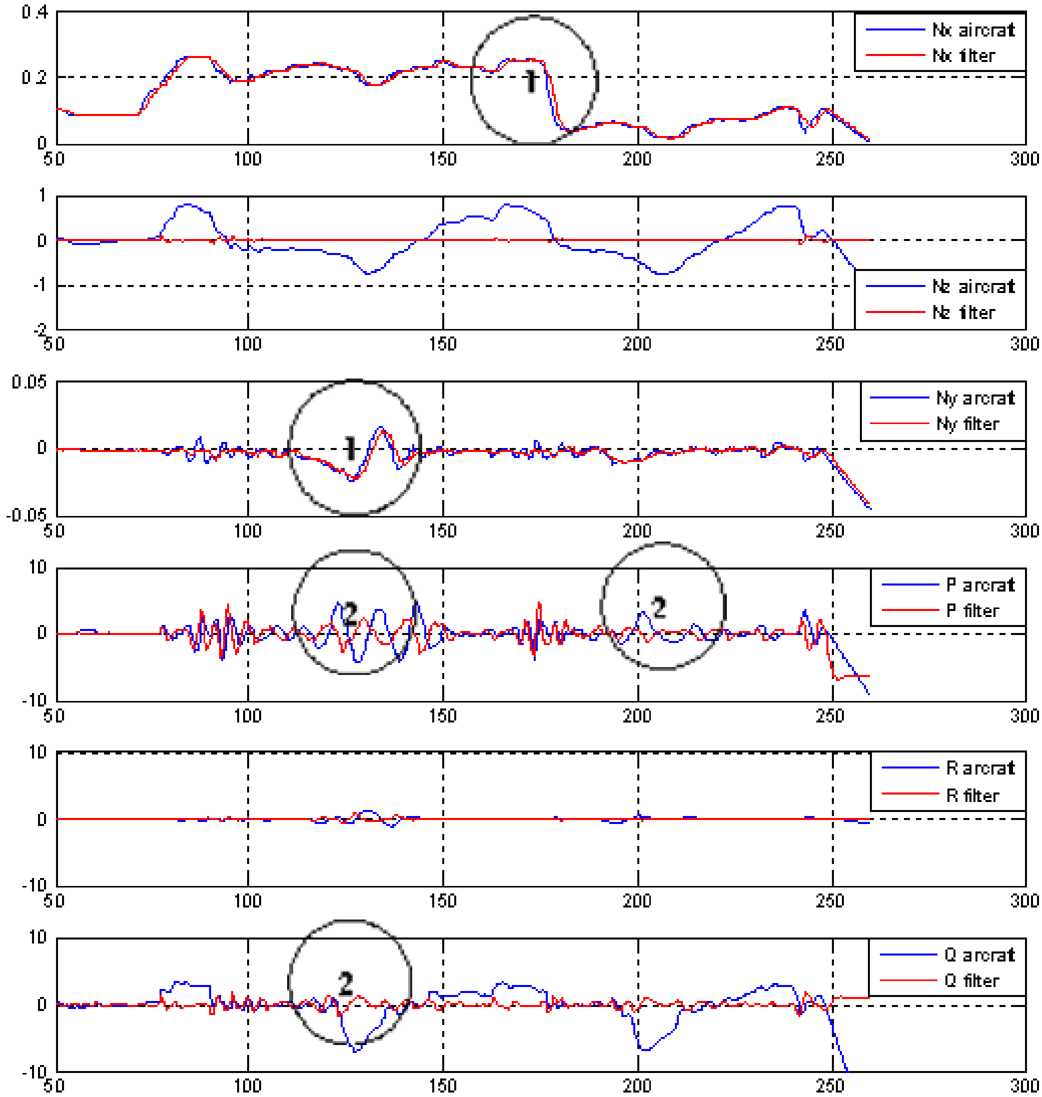

Fig. 5. Comparison of the aircraft motion and “classical” filters’ outputs.

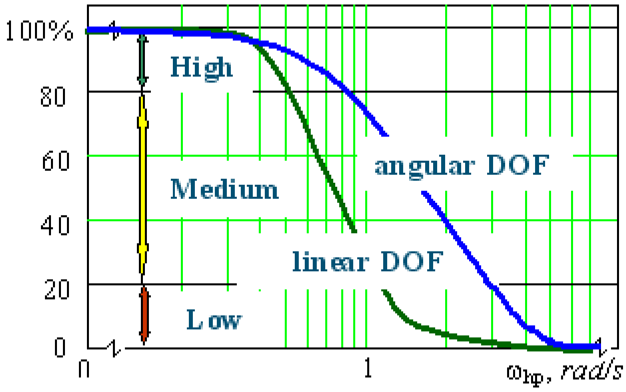

Fig. 6. Motion fidelity criteria to select high-pass filter frequencies.

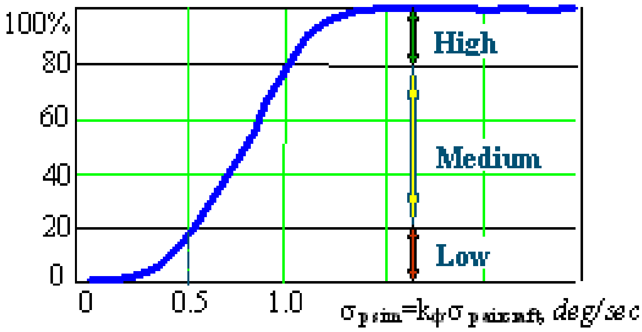

Fig. 7. Motion fidelity criteria to select gains.

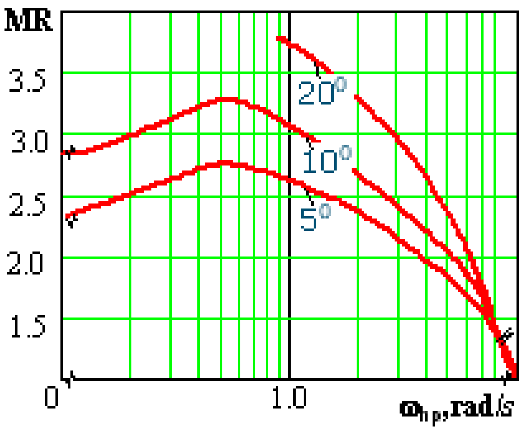

Fig. 8. Motion fidelity criteria to avoid false cues in angular motion reproduction.

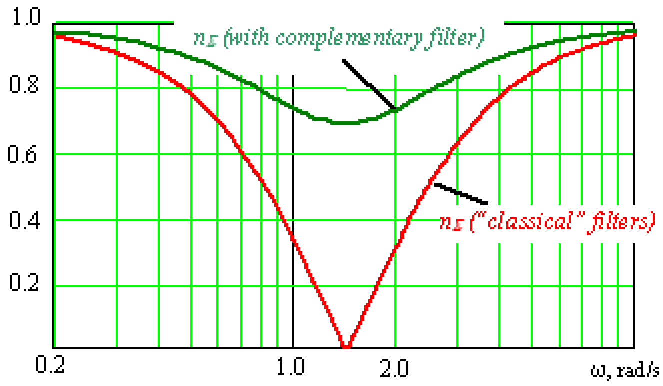

Fig. 9. Minimization of phase distortion in lateral acceleration reproduction.

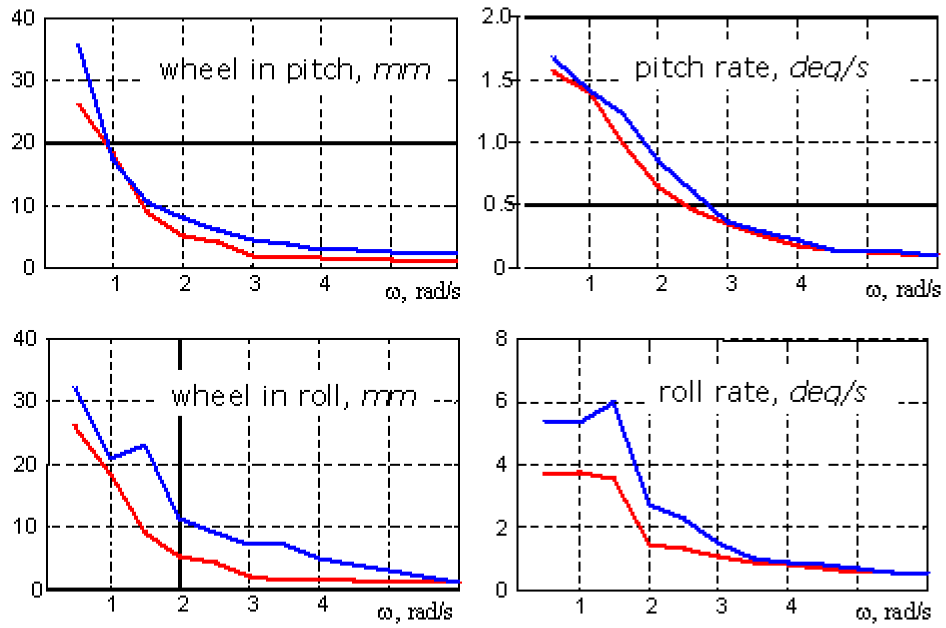

Fig. 10. Spectra of the wheel displacements and controlled parameters for motion-off (in blue) and motion-on (in red) cases; one pilot, one upset scenario.

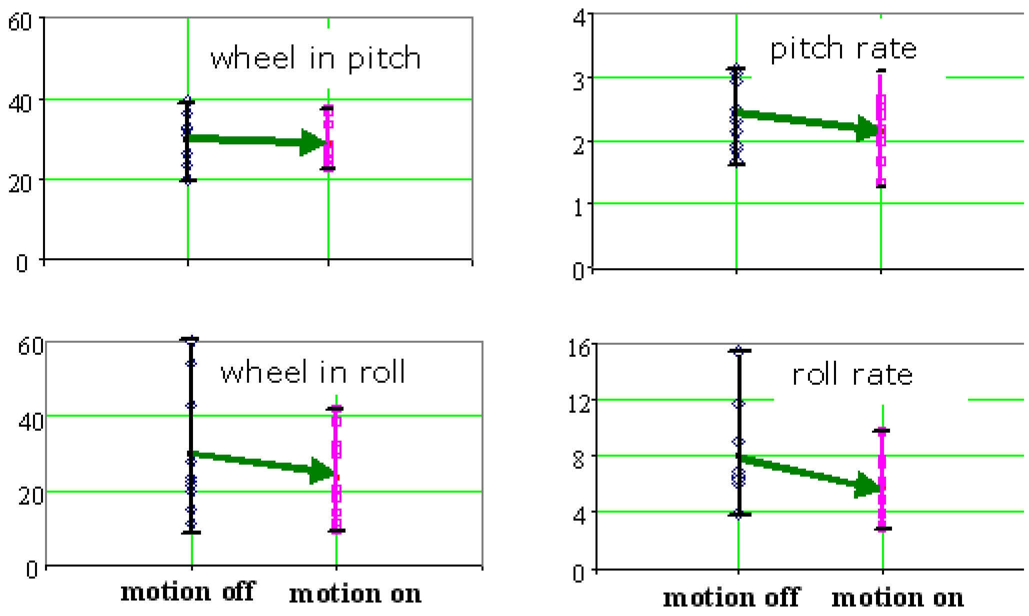

Fig. 11. Standard deviations of wheel displacements and controlled parameters for motion-off and motion-on cases (one pilot, one upset scenario).

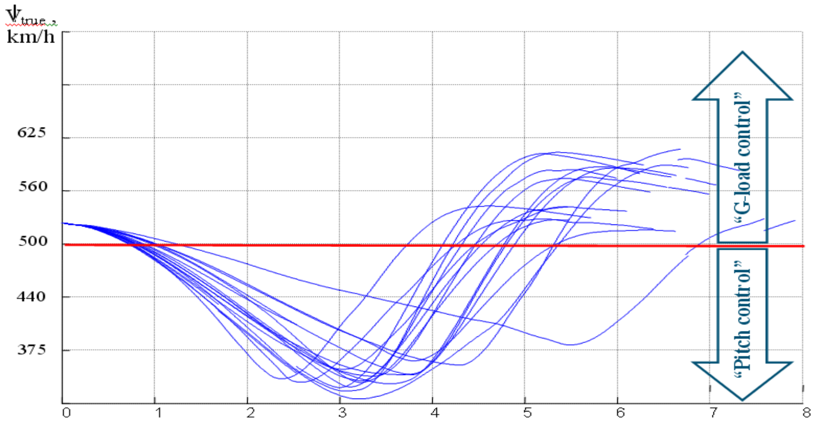

Fig. 12. The flight velocities in upset/stalls and upset recovering (different upset/stall scenarios).